23rd Australasian Fluid Mechanics Conference – 23AFMC
Sydney, Australia
4-8 December 2022
Paper No: AFMC2022-216

Evaporation Modelling of Refrigerant-Solvent Droplets

Harry N. Scott [1], Swetha C. Vutlapalli [1], Damon R. Honnery [1] and Daniel J. Duke [1*]

[1] LTRAC Dept. of Mechanical and Aerospace Engineering, Monash University, Clayton, VIC 3800, Australia

* Email: daniel.duke@monash.edu

Abstract

Refrigerants are volatile at ambient temperatures. Their application as propellants in flash-atomising sprays is common, particularly in medical sprays. Lower volatility solvents are often blended, forming binary component spray droplets. An effective conductivity model was developed to characterise the evaporation of these blended droplets. The effects of propellant type, diffusivity and initial composition are presented here. When rapidly mixing, evaporation is described by 4 stages: (I) droplet heating/cooling, (II) refrigerant vaporisation, (III) secondary droplet heating and (IV) ethanol vaporisation. As mixing reduces, the droplet vaporisation is limited by the rate of propellant transport to the surface. Consequently, the evaporation stages II-IV occur simultaneously. Both liquid species evaporate concurrently, and propellant remains trapped in the droplet core. This occurs at diffusivities with an order of magnitude of 10^{-9} m^2s^{-1}. Larger initial ethanol concentrations increase the duration of concurrent species evaporation. Analysis of propellant type highlights the importance of improving thermodynamic data tables for refrigerant ethanol blends. The thermodynamic properties not only influence the evaporation within stages but also affect which processes dominate. When designing formulations, the entire evaporation process must be examined.

Nomenclature

c_P	Specific Heat	Z	Dimensionless Temperature	Nu	Nusselt Number	0	Initial
D	Mass Diffusivity	α	Thermal Diffusivity	Pr	Prandtl Number	HFA	Refrigerant
r	Radial Location	β	Dimensionless Quantity	Re	Reynolds Number	eth	Ethanol
r_s	Dimensionless Droplet Radius	ξ	Dimensionless Radius	Sc	Schmidt Number	l	Liquid
R	Droplet Radius	τ	Dimensionless Time	Sh	Sherwood Number	v	Vapour
t	Time	χ	ETC Coefficient			∞	Ambient
T	Temperature	B_M	Heat and Mass Spalding Numbers	*Subscripts*		D	Diameter
Y	Mass Fraction	F_M	Heat and Mass Correction Factors	i	Species		
U	Relative droplet velocity	Le	Lewis Number	s	Surface		

1. Introduction

Regulations on global emissions necessitate the transition away from high global warming potential (GWP) refrigerants such as HFA134a (Pritchard 2022). For many applications the refrigerant's high vapour pressure at ambient temperatures is critical. This includes flash atomising sprays, a process used to create droplets in pressurised metered dose inhalers (pMDIs). Potential low GWP replacements for HFA134a in pMDIs are HFA152a and HFA1234ze(E) (Pritchard 2022).

Within pMDI droplets, drug is dissolved. Pharmaceutical compounds have low solubility in Hydrofluorocarbons (Newman 2005). The addition of a liquid cosolvent to the refrigerants is required

to achieve adequate concentrations of solute within the droplets. This cosolvent is typically ethanol, at typical concentrations of up to 20% (Mydral *et al.* 2014). Vapour pressure differences between ethanol and refrigerants are approximately two orders of magnitude (NIST, 2022). With a substantial vapour pressure difference between components, droplet evaporation will be significantly affected. The impact that formulation has on this multicomponent evaporation process must be quantified. The dominant evaporation mechanisms within these binary mixtures, however, are poorly understood.

Experimental investigations of refrigerant droplets are challenging. Droplet size, velocity, and number density within sprays limit laser-based techniques (Duke *et al.* 2015). Isolated droplet investigations are possible; however, short timescales and low temperatures restrict the investigation domain (Scott *et al.* 2022). Spectroscopic measurements that quantifying internal droplet composition are not applicable for these blends as evaporation timescales are too short (Reid *et al.* 2007).

Computational modelling avoids the numerous issues associated with experimental droplet research. The evaporation can be isolated from the spray formation process (Sirignano 1999). This allows investigations into the dominant processes within droplet evaporation event. Computational modelling does however have other limitations. Inaccuracy within simulations can result from poor quality thermodynamic data, and the simplification of physical mechanisms. Refrigerant ethanol blends have limited experimental thermodynamic data. This restricts the overall possible accuracy of evaporation models, especially when considering the non-ideal nature of the mixture. A simplified reduced order model was therefore selected to investigate the evaporation of refrigerant ethanol droplets. The low computing cost allows for extensive parametric sweeps (Sirignano 1999), determining the sensitivity to some key formulation parameters.

Reduced order models are commonly used to simulate fuel droplet evaporation (Sazhin *et al.* 2006). Within fuel sprays the far field is of greater significance with combustion performance being the driving metric. The mixtures also have similar volatilities. For refrigerant ethanol droplets, the liquid phase and consequential effects on drug formation are of greater significance and volatility difference between species is large. A mixing model in the liquid phase is required to investigate the effects of the formulation. An effective conductivity model has shown reasonable accuracy for other binary mixtures and so was selected for this study (Sazhin *et al.* 2010).

This model approximates convection within the liquid phase by modifying the diffusion equation. The equation relies on a diffusivity coefficient, a measure of the diffusion rate between two species. There is no available value in literature for refrigerant ethanol mixtures. The sensitivity to this parameter must therefore be investigated. For comparison a typical value for ethanol and water is approximately 0.84×10^{-9} $m^2 s^{-1}$ (Cussler 2009).

The work presented here investigates the effect of propellant type, composition, and diffusivity of ethanol-refrigerant droplet evaporation. The novelty of this work lies in the properties of the specific mixtures considered, which differ to those used in previous simulations of this type. The initial conditions match experimental conditions from Scott *et al.* (2022) for future model validation. This will support the transition to lower polluting propellants and improved application performance.

2. Methodology

An effective conductivity model was developed to simulate the evaporation of refrigerant-solvent droplets. The droplet was broken up into 3 regions: liquid phase, vapour boundary layer and far field vapour phase. The liquid phase solved modified diffusion equations to determine composition and temperature. It allowed for large concentration gradients with species volatility difference approximately 2 orders of magnitude (NIST 2022). The gas phase region near the surface was developed using the boundary layer conservation equations (Sirignano, 1999). Far field vapour was assumed uniform and was not the focus of this study. Droplet diameter and evaporation timescales were small in comparison to typical far field fluctuations.

Singular spherical, supercooled droplets vaporised whilst falling with a vertical trajectory. A steady, isothermal counterflow of dry air increased the convective heat transfer. Wake effects were ignored as droplet Reynolds number is less than 200 for all simulations. Initial and boundary

conditions (Table 1) matched experimental conditions from Scott *et al.* (2022). This enables future experimental validation work.

The effects of propellant type, ethanol concentration and diffusion coefficient were investigated. HFA134a, HFA152a and HFA1234ze(E) were utilised as the refrigerants. Ethanol was selected as the solvent. The selection of these mixtures reflects typical pharmaceutical spray droplets (Mydral *et al.* 2014). Thermodynamic data was sourced from REFPROP (NIST 2022) unless otherwise stated. A sample of relevant thermodynamic properties are listed in Table 2.

Property	Value(s)	Property	Value(s)
Initial Droplet Temperature [ºC]	-45	Initial Ethanol Mass Fraction	0 - 0.5
Counterflow temperature [ºC]	193	Mass diffusion coefficient [m^2s^{-1}]	$1x10^{-5}$-$1x10^{-9}$
Initial droplet velocity [m s^{-1}]	3.73	Initial droplet diameter [μm]	315
Counterflow velocity	-0.864		

Table 1: Simulation initial and boundary conditions.

Propellant	HFA134a	HFA152a	HFA1234ze
Heat of vaporisation [kJ/kg]	230	349	211
Density [kg m^{-3}]	1435	1056	1365
Specific Heat [kJ/kg]	1.24	1.57	1.24
Vapour pressure [kPa]	36.7	34.0	26.1

Table 2: Sample of relevant thermodynamic properties at 227K (NIST, 2022).

Droplet position and velocity were calculated using a force balance of gravity and drag. A drag coefficient correlation was applied (Brauer 1973) with Reynolds number limited to a minimum of 0.025. The internal surface velocity, Re, Sc, Pr and Pe numbers were calculated using the method found in Sirignano (1999).

Heat and mass transfer in the liquid phase were modelled using the normalised radial diffusion equations (Sirignano, 1999) given in equation (1). $\Phi = \mathrm{Y_i}$ and $\Omega = D_l$ in the mass equations, whilst $\Phi = Z$ and $\Omega = \alpha_l$ for the heat equation. The droplet was discretised using 100 radial grid points. Node spacing was parabolic with refinement at the droplet centre and surface. Time stepping was dependant on the gradient of species evaporation fraction and diffusivity. The non-uniform discretisation minimised numerical instability and maintained computational efficiency. A Backwards Euler method propagated the differential equations forward in time, maximising stability.

$$\frac{\alpha_{l,0}}{\Omega}\left(r_s^2\frac{\partial\Phi}{\partial\tau}-\beta\xi\frac{\partial\Phi}{\partial\xi}\right)=\chi_\Omega\left(\frac{\partial^2\Phi}{\partial\xi^2}+\frac{2}{\xi}\frac{\partial\Phi}{\partial\xi}\right),\ \Phi=\mathrm{Y_i},Z,\ \Omega=D_l,\alpha_l \tag{1}$$

$$\xi=\frac{r}{R(t)},\ Z=\frac{T_l(r,t)-T_{l,0}}{T_{l,0}},\ r_s=\frac{R(t)}{R_0},\ \beta=\frac{1}{2}\frac{dr_s}{d\tau},\ \tau=\frac{\alpha_{l,0}t}{R_0^2} \tag{2}$$

Heat and mass diffusion were modified using an effective conductivity coefficient χ. Through increasing the diffusion rate, an improved approximation of the droplet mixing was made. This effective coefficient estimated the additional mixing from convective effects using correlations from Abramzon & Sirignano (1989).

Zero gradient boundary conditions were applied at the droplet centre. A first law energy balance correlated the temperature diffusion, convective heat flux and latent heat absorption at the surface. Similarly, species mass flux was equated to the concentration gradient using Fick's first law.

The surface heat and mass flux were determined at each time step. These were calculated from an analysis of the vapour phase. The gas phase assumed only outward mass transfer. Firstly, vapour pressure of each species was determined. The correlation from Gavtash *et al.* (2015) was utilised for all refrigerant ethanol blends. No other readily available thermodynamic data exists for HFA152a or HFA1234ze(E) blends with ethanol. This highlights the importance of determining sensitivity to various thermodynamic properties.

By combining Raoult's and Dalton's law the partial pressures of each species were determined. This gives the vapour mass fractions and species fractional evaporation at the surface. Vapour temperature near the surface was determined using the 1/3 rule (Yuen & Chen 1976). Updated thermodynamic properties were calculated for the new temperatures and vapour compositions. Mixture values were calculated (Polling *et al.* 2001). Vapour diffusivity was estimated using Lennard-Jones parameters (Bird *et al.* 1960). Relevant heat and mass transfer dimensionless numbers were calculated using correlations from previous studies (Clift *et al.* 1978) (Honnery *et al.*, 2013) (Abramzon & Sirignano, 1989). The relevant heat transfer numbers were solved iteratively. The equations below account for Stefan flow effects on the boundary layer and empirical corrections to solutions of the relevant boundary layer conservation equations (Sirignano 1999).

$$B_M = \frac{(Y_{v,s,HFA}+Y_{v,s,eth})-(Y_{v,\infty,HFA}+Y_{v,\infty,eth})}{1-Y_{v,s,HFA}-Y_{v,s,eth}} \tag{3}$$

$$B_T = (1 + B_M)^{\frac{c_{P,l}\, Sh\, B_M \log(1+B_T)}{Le\, c_{P,v}\, Nu\, B_T \log(1+B_M)}} - 1 \tag{4}$$

$$F_n = (1 + B_n)^{0.7} \frac{\log(1+B_n)}{B_n},\ B_n = M, T \tag{5}$$

$$Sh = 2\left(\frac{\log(1+\mathrm{B_M})}{\mathrm{B_M}}\right)\left(1 + \frac{(1+\mathrm{Re_D Sc})^{\frac{1}{3}}\max([1,\mathrm{Re}_D^{0.077}])-1}{2\mathrm{F_M}}\right) \tag{6}$$

$$Nu = 2\left(\frac{\log(1+B_T)}{B_T}\right)\left(1 + \frac{(1+Re_D Pr)^{\frac{1}{3}}\max([1,Re_D^{0.077}])-1}{2F_T}\right) \tag{7}$$

The convective heat flux was modelled using the Nusselt number correlation from Equation (7). The mass flux was given by Equation (8) (Sazhin *et al.* 2010). Using Eulerian time stepping the updated droplet mass and radius were determined. These were applied to the diffusion equations and the solution marched forward. This algorithm was iterated until less than 0.4% of the original mass remained. Cumulative error prevents further evaporation in some diffusion limiting cases.

$$\dot{m}_l = -2\pi \mathrm{R(t)} \mathrm{f_i} \rho_{\mathrm{BL}} \mathrm{D_v} \mathrm{B_M} \mathrm{Sh} \tag{8}$$

3. Results

3.1 Refrigerant Effects

To analyse refrigerant effects, an intermediate mass diffusivity coefficient of $1\text{x}10^{-8}$ $\mathrm{m^2 s^{-1}}$ is assumed. Droplet composition is set to 15% ethanol by mass. Radius and surface temperature evolution are illustrated in Figure 1. This describes typical ETC droplet model behaviour for refrigerant ethanol formulations. Each propellant-solvent mixture exhibits a phase change process characterised by four distinct stages: (I) droplet heating/cooling, (II) refrigerant vaporisation, (III) secondary droplet heating and (IV) ethanol vaporisation.

The propellant effects on evaporation are compared in Figure 1. No monotonic trends between propellants are observed over the entire droplet lifespan. Instead, each evaporation stage is influenced separately by each propellant's unique properties. As surface composition within the droplet evolves, different thermodynamic processes dominate. The propellant not only affects this concentration change, but also the thermodynamic properties governing the dominant mechanisms within each stage. The dominant processes of each stage are discussed.

Stage I is characterised by the rapid change initial surface temperature. Here, surface temperature adjusts from initial temperature to the requisite conditions for quasi-steady propellant evaporation. Stabilisation of the surface temperature is achieved when evaporative cooling is balanced by

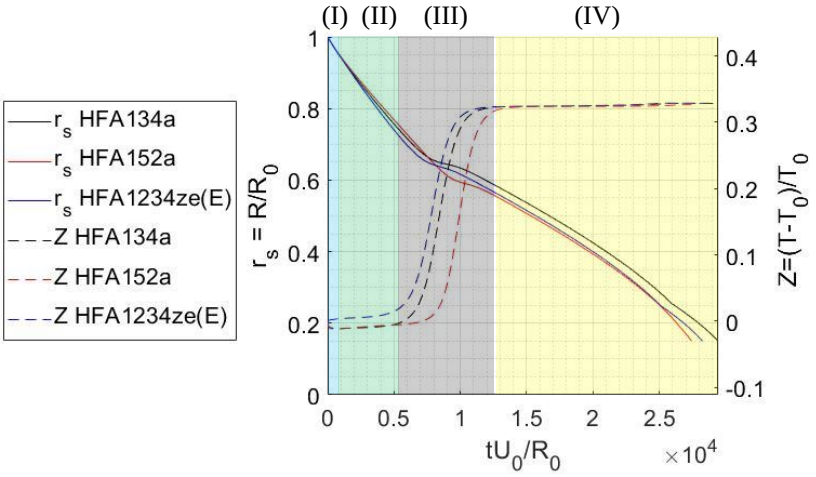

Figure 1: Normalised droplet radius (left axis, solid lines) and dimensionless surface temperature (right axis, dotted lines) vs dimensionless time. The four stages of the evaporation process are labelled and coloured: (I, blue) droplet heating/cooling, (II, green) refrigerant vaporisation, (III, red) secondary droplet heating, (IV, yellow) ethanol vaporisation.

convective heat transfer. This quasi-steady surface temperature is dictated by the propellant's vapour pressure. Larger vapour pressures reduce surface temperature, reflected in Table 2 and Figure 1.

Stage II is defined by isothermal, quasi-steady evaporation of refrigerant. The duration of this stage is regulated by the surface composition, temperature difference between phases and latent heat of vaporisation. Assuming constant diffusivity across mixtures ensures surface composition is similar for each propellant. Temperature difference between phases is similar for all propellants, depicted in Figure 1. Therefore, latent heat effects dominate. The quasi-steady evaporation stage (II) is significantly longer than the initial heating/cooling stage (I). Consequently, the propellant in HFA1234ze(E) droplets fully vaporises before HFA152a and HFA134a. This result is unexpected given that HFA1234ze(E) has the lowest vapour pressure.

Stage III is defined by the significant increase in surface temperature on Figure 1. The increase in surface ethanol concentration (Figure 2) reduces mixture vapour pressure. Propellant vaporisation is limited by surface availability and diffusion rate of refrigerant. Sensible heat transfer and droplet temperature increase. The radius when secondary heating commences is dependent on the propellant density. Larger propellant densities increase initial ethanol mass, with fixed initial radii and initial composition. Increasing surface temperature elevates ethanol vapour pressure. With steadily growing vapour pressure ethanol evaporation rate increases. Latent heat transfer eventually surpasses specific heat transfer and droplet surface temperature stabilises.

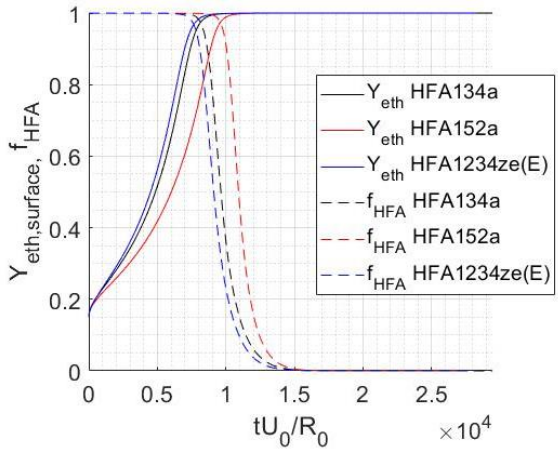

Figure 2: Liquid surface mass fraction (solid) and evaporative fraction (dashed) vs dimensionless time.

Stage IV commences with a second instance of quasi-steady evaporation. This isothermal surface temperature is independent of propellant. Surface temperature is determined by ethanol vapour pressure. Stage duration is determined by initial ethanol mass, dependant on propellant density. The

evaporation rate in stage IV is substantially reduced compared to stage II due to the lower relative volatility of ethanol. Consequently, stage IV is the longest evaporation stage. Refrigerant evaporation rate is negligible as the propellant fully vaporised in the preceding stages (Figure 2).

Overall, the effect of propellant type on evaporation is complex. The interaction of propellant properties not only changes with propellant type, but critically the dominance of these parameters varies with concentration such that the controlling properties may change during the evaporation event itself. Latent heat, diffusivity, liquid density and vapour pressure influence the various stages of evaporation differently. Replacing refrigerants with matching vapour pressure will not yield the same evaporation profile. This highlights the need for careful consideration of the entire evaporation process when designing new formulations. Accurate thermodynamic data for these non-ideal mixtures is critical, enabling improved application designs.

3.2 Diffusivity Effects

Results for HFA152a ethanol blends are presented. Similar trends are observed for other propellant solvent mixtures. Diffusion coefficients of fluids range from 10^{-5} to 10^{-10} m^2s^{-1} (Cussler 2009) depending on mixture and phase. The diffusion coefficient of propellant ethanol blends at low temperatures is unknown. A wide range of diffusion coefficients is examined to determine the significance of this property on evaporation.

For diffusion coefficients less than 10^{-7} m^2s^{-1}, liquid phase mass transfer is effectively instantaneous. Here, droplet convection or diffusion timescales are significantly smaller than evaporative timescales. The model approaches the infinite diffusion limit. Stage II allows for the complete evaporation of refrigerant before droplet temperature increases. This is shown in Figure 3a where the gradient of f_{eth} is large when it increases from 0 to 1.

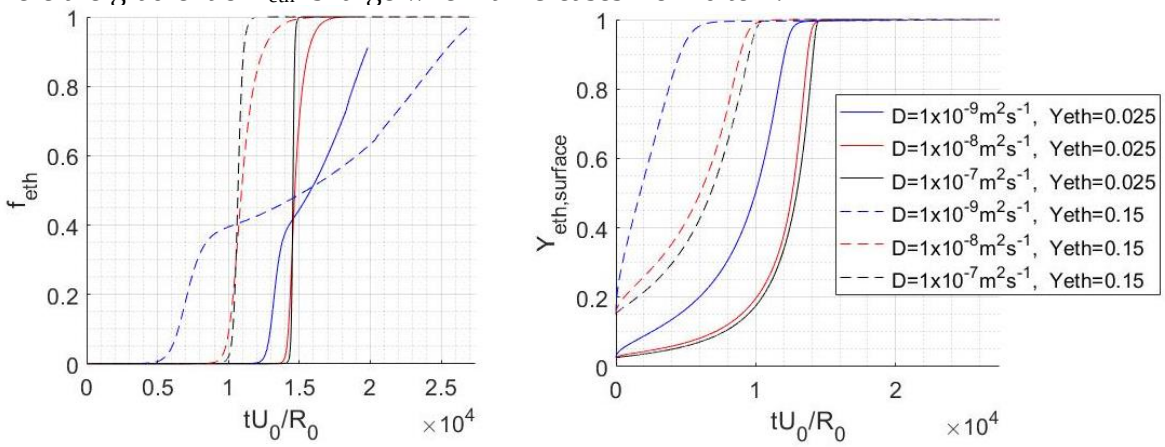

Figure 3: (a) Species evaporation fraction vs dimensionless time for two initial ethanol concentrations. (b) Liquid surface ethanol mass fraction vs dimensionless time for two initial ethanol concentrations.

For diffusion coefficients of 10^{-9} m^2s^{-1}, a limiting of liquid propellant transport to the surface is observed. The rate of surface ethanol enrichment increases, shown in Figure 3b. The low concentration of surface propellant results in diffusion limited evaporation. Here, vaporisation rate of propellant is entirely dependent on the diffusion rate rather than heat transfer. Stages II-IV of the evaporation process are significantly affected shown in Figure 4.

After initial enrichment of ethanol at the surface, diffusion rate of propellant controls the evaporation of this species. The reduced latent heat absorption expedites the secondary heating stage (III). Whilst propellant continues to vaporise surface temperature increases, observed in Figure 4. This increases ethanol vapour pressure and simultaneous species evaporation occurs, demonstrated by the reduction in the gradient of f_{eth} in Figure 3a.

The diffusion or effective mixing rate influences the entire evaporation process. If on the order of 10^{-9} m^2s^{-1} the vaporisation of propellant is diffusion limited. This results in a spatial and temporal droplet composition that significantly differs to what was observed in section 3.1. With reduced mixing, evaporation stages occur simultaneously. Values of $0.84x10^{-9}$ m^2s^{-1} have been estimated for ethanol in water (Cussler 2009) and so diffusion limited evaporation of refrigerant ethanol blends

may have this order of magnitude. Obtaining experimental diffusion rates for these formulations is necessary. If diffusion limited, accurate determination of this value is critical to the ETC model as it controls the evaporation rate of propellant.

Diffusion effects on refrigerant type, further complicate the evaporation. The relative importance of thermodynamic mechanisms is no longer as obvious when compared to results from section 3.1. With refrigerants having significantly different molecular weights and chemical structures the diffusivities may vary substantially. This highlights the need to consider the entire evaporation process for each propellant blend as the dominance of each mechanism will depend on formulation.

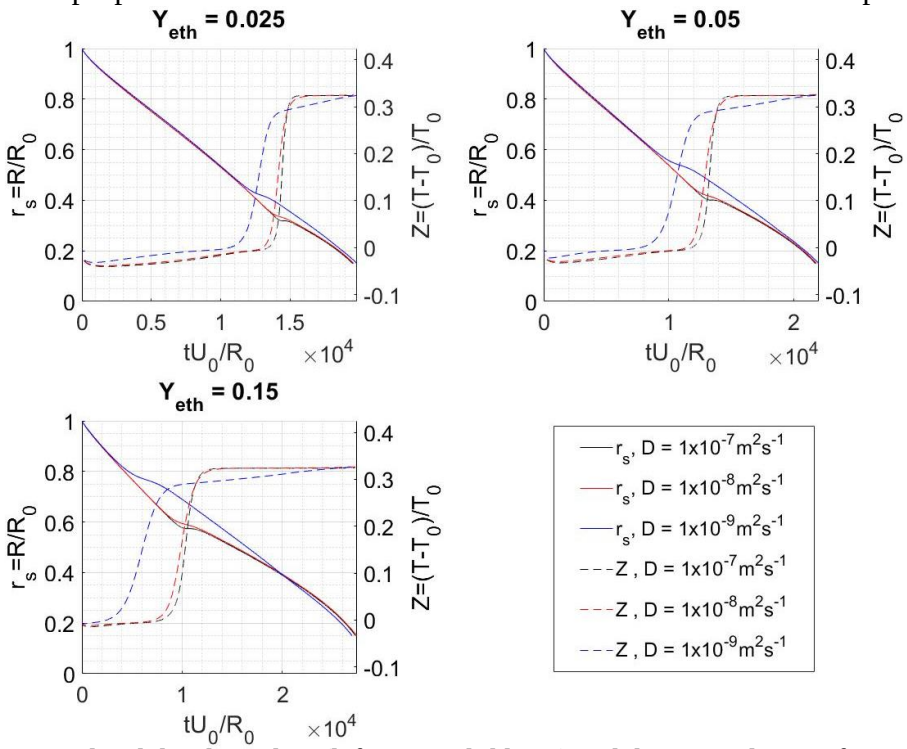

Figure 4: Normalised droplet radius (left axis, solid lines) and dimensionless surface temperature (right axis, dashed lines) vs dimensionless time.

3.3 Initial Ethanol Concentration Effects

The influence of initial composition on droplet radius and surface temperature is observed in Figure 4. The distinct evaporation stages are exhibited for all compositions with diffusivities of 10^{-7}-10^{-8} m^2s^{-1}. Here, the initial concentration of ethanol predominantly affects the duration of the quasi-steady evaporation stages (II, IV).

Initial composition impacts the entire vaporisation event when evaporation is diffusion limited. Increasing initial ethanol concentration expedites the occurrence of diffusion limited evaporation, shown in Figures 3 and 4. Surface composition adjusts more rapidly resulting in prolonged evaporation of propellant. Consequently, the radial profiles in Figure 4 exhibit more significant differences at higher ethanol concentrations.

The effects of refrigerant type and diffusivity are both influenced by the initial concentration. This reiterates the importance of interactions between evaporation mechanisms when species volatility differences are several orders of magnitude. Independent considerations of droplet evaporation are required for each formulation, with no clear monotonic trends. The need for accurate thermodynamic data within these non-ideal mixtures is critical to ensure future application performance is maximised.

4. Conclusions

An effective conductivity model was developed to investigate the evaporation of refrigerant ethanol droplets. The effect of refrigerant type, diffusivity and initial composition were studied. In cases of rapid mixing, the evaporation is characterised by 4 distinct stages: (I) droplet heating/cooling, (II) refrigerant vaporisation, (III) secondary droplet heating and (IV) ethanol vaporisation. Different

mechanisms control each evaporation stage. These are dependent on latent heat, liquid density, and vapour pressure. In lower diffusion simulations, the evaporation process is diffusion or mixing limited. Evaporation stages (II-IV) are observed to occur simultaneously. When diffusion limited the diffusivity value is critically important as it controls evaporation rate and droplet composition. When acting as a solvent, solute concentration within the ethanol controls particle formation. With simultaneously evaporating species, particle formation could be influenced by the diffusion or mixing within the droplet. Obtaining accurate thermodynamic data for these non-ideal mixtures is essential in developing new formulations. The interaction thermodynamic properties not only change between propellants, but critically the dominant mechanisms themselves may change during the evaporation event itself. This highlights the need to consider each formulation separately with no clear monotonic trends between propellants.

Acknowledgments

We acknowledge funding support from the Australian Research Council (DP200102016) (LP190100938) and Kindeva Drug Delivery.

References

Abramzon, B. & Sirignano W.A. 1989, Droplet vaporization model for spray combustion calculations, *International J of Heat and Mass Transfer*, **32**(9), 1605-1618.

Bird, R., Stewart, W. & Lightfoot, E. 1960, *Transport Phenomena*, New York, John Wiley & Sons.

Brauer, H. 1973 Momentum, mass, and heat-transfer through boundary surface of spherical-particles. *Chemie Ingenieur Technik*, **45**(18), 1099-1103.

Clift, R., Grace, J. & Weber, M. 1978, *Bubbles, drops, and particles,* New York, Academic Press.

Cussler, E. 2009, *Diffusion: mass transfer in fluid systems, 3rd ed.* Cambridge University Press

Duke, D.J. 2015, A Review of Synchrotron Radiation Diagnostics for Fluid Mechanics, in *7th Australian Conference on Laser Diagnostics in Fluid Mechanics and Combustion*, 15-22.

Gavtash, B., Myatt, B., O'Shea, H., Mason, F., Lewis, D., Church, T., Versteeg, H., Hargrave, G. & Brambilla, G. 2016, Saturated vapour pressure (SVP) measurement of ethanol/HFA binary mixtures. *Journal of Aerosol Medicine and Pulmonary Drug Delivery*.

Honnery, D., Nguyen, D. & Soria, J. 2013, Microdroplet evaporation under increasing temperature conditions: Experiments and modelling, *Fuel*, **105**, 247-257.

Lemmon, E.W., Bell, I.H., Huber, M.L. & McLinden, M.O. NIST Standard Reference Database 23: Reference Fluid Thermodynamic and Transport Properties-REFPROP, Version 10.0, National Institute of Standards and Technology, Standard Reference Data Program, Gaithersburg, 2018.

Myrdal, P.B., Sheth, P. & Stein S.W. 2014, Advances in metered dose inhaler technology: formulation development, *AAPS PharmSciTech* **15**(2),434-55.

Newman, S. 2005, Principles of Metered-Dose Inhaler Design, *Respiratory Care*, **50** (9) 1177-1190.

Polling B.E., Prausnitz J.M. & O'Connell J.P. 2001, *The Properties of Gases and Liquids 5th Edition*, New York, McGraw-Hill Education.

Pritchard, J. 2022, Is the Climate Right for a New pMDI Propellant?, *Respiratory Drug Delivery*

Reid, J., Meresman, H., Mitchem, L., & Symes, R., 2007, Spectroscopic studies of the size and composition of single aerosol droplets, *International Reviews in Physical Chemistry*, **26**(1)

Sazhin, S.S., Kristyadi, T., Abdelghaffar, W.A. & Heikal M.R. 2006, Models for fuel droplet heating and evaporation: Comparative Analysis, *Fuel*, **85**(12) 1613-1630

Sazhin, S., Elwardany, A., Krutitskii, P., Castanet, G., Lemoine, F., Sazhina, E. & Heikal, M. 2010, A simplified model for bi-component droplet heating and evaporation. *International Journal of Heat and Mass Transfer*, **53**(21-22), 4495-4505.

Sirignano, W. 1999, *Fluid dynamics and transport of droplets and sprays*, Cambridge University.

Scott, H., Nguyen, D., Honnery, D. & Duke, D. 2022, The production and evaporation of HFA152a Droplets from the Plateau-Rayleigh Instability, *12th AHMTC.*

Yuen, M. & Chen, L. 1976, On Drag of Evaporating Liquid Droplets, *Combustion Science and Technology*, **14**(4-6), 147-154.